



Monoclonal Antibody Therapy against *Acinetobacter baumannii*

Travis B. Nielsen,^{a,b,c} Jun Yan,^c Matthew Slarve,^c Peggy Lu,^c Rachel Li,^c Juan Ruiz,^c Bosul Lee,^c Elizabeth Burk,^c Yuli Talyansky,^c Peter Oelschlaeger,^d Kyle Hurth,^e William Win,^e Brian M. Luna,^c Robert A. Bonomo,^{f,g,h} Brad Spellbergⁱ

^aStritch School of Medicine, Loyola University Chicago, Maywood, Illinois, USA

^bParkinson School of Health Sciences and Public Health, Loyola University Chicago, Maywood, Illinois, USA

^cDepartment of Molecular Microbiology & Immunology, Keck School of Medicine at the University of Southern California, Los Angeles, California, USA

^dDepartment of Pharmaceutical Sciences, College of Pharmacy, Western University of Health Sciences, Pomona, California, USA

^eDepartment of Pathology, Keck School of Medicine at the University of Southern California, Los Angeles, California, USA

^fLouis Stokes Cleveland Department of Veterans Affairs Medical Center, Cleveland, Ohio, USA

^gDepartment of Medicine, Case Western Reserve University, Cleveland, Ohio, USA

^hDepartments of Pharmacology, Molecular Biology and Microbiology, Biochemistry, and Proteomics and Bioinformatics, Case Western Reserve University, Cleveland, Ohio, USA

ⁱLos Angeles County and University of Southern California Medical Center, Los Angeles, California, USA

ABSTRACT Extremely drug-resistant (XDR) *Acinetobacter baumannii* is a notorious and frequently encountered pathogen demanding novel therapeutic interventions. An initial monoclonal antibody (MAb), C8, raised against *A. baumannii* capsule, proved a highly effective treatment against a minority of clinical isolates. To overcome this limitation, we broadened coverage by developing a second antibody for use in a combination regimen. We sought to develop an additional anti-*A. baumannii* MAb through hybridoma technology by immunizing mice with sublethal inocula of virulent, XDR clinical isolates not bound by MAb C8. We identified a new antibacterial MAb, 65, which bound to strains in a pattern distinct from and complementary to that of MAb C8. MAb 65 enhanced macrophage opsonophagocytosis of targeted strains and markedly improved survival in lethal bacteremic sepsis and aspiration pneumonia murine models of *A. baumannii* infection. MAb 65 was also synergistic with colistin, substantially enhancing protection compared to monotherapy. Treatment with MAb 65 significantly reduced blood bacterial density, ameliorated cytokine production (interleukin-1 β [IL-1 β], IL-6, IL-10, and tumor necrosis factor), and sepsis biomarkers. We describe a novel MAb targeting *A. baumannii* that broadens immunotherapeutic strain coverage, is highly potent and effective, and synergistically improves outcomes in combination with antibiotics.

KEYWORDS *Acinetobacter baumannii*, XDR, carbapenem resistant, monoclonal antibody, immunotherapy

More than 75,000 cases of extremely drug-resistant (XDR) *Acinetobacter baumannii* infections occur annually in developed countries, resulting in more than 30,000 deaths and excess health care costs of \$742 million (1). One-third of those cases occur in the United States, resulting in 10,000 deaths and health care costs of \$390 million every year (1). More than half of *A. baumannii* isolates from the United States and China are XDR (1–4), yet, unlike other resistant bacteria that cause deadly infections, there are few antibiotics in the pipeline that could treat these infections (5, 6). Thus, there is a critical need for new strategies to prevent and treat these infections.

We previously found that virulent *A. baumannii* strains can evade the innate immune system, causing sustained TLR4 ligation by lipopolysaccharide (LPS), which ultimately leads to death by sepsis (7–10). Thus, enhancing innate immunity is a

Citation Nielsen TB, Yan J, Slarve M, Lu P, Li R, Ruiz J, Lee B, Burk E, Talyansky Y, Oelschlaeger P, Hurth K, Win W, Luna BM, Bonomo RA, Spellberg B. 2021. Monoclonal antibody therapy against *Acinetobacter baumannii*. *Infect Immun* 89:e00162-21. <https://doi.org/10.1128/IAI.00162-21>.

Editor Denise Monack, Stanford University

Copyright © 2021 American Society for Microbiology. All Rights Reserved.

Address correspondence to Travis B. Nielsen, travis.nielsen@gmail.com.

Received 18 March 2021

Returned for modification 21 April 2021

Accepted 6 July 2021

Accepted manuscript posted online 26 July 2021

Published 16 September 2021

promising strategy to improve outcomes. Therefore, we focused on monoclonal antibodies (MAbs) as a passive immunotherapeutic approach, first demonstrating that passive immunization with polyclonal serum targeting *A. baumannii* improved survival of infected recipient mice, validating the approach (9).

To that end, we previously developed a MAb, C8, that was able to bind approximately half of *A. baumannii* strains tested (11). Here, we present a second MAb, 65, that is also highly protective during blood and lung infections, complementing the strain coverage of our first MAb. We describe *in vitro* and *in vivo* antibacterial effects of MAb 65, demonstrating efficacy with a humanized variant of the MAb, supporting translation of both MAbs to treat drug-resistant *A. baumannii* infections.

RESULTS

Development and characterization of anti-*A. baumannii* IgG1 MAb. We generated a murine IgM MAb with a kappa light chain through hybridoma technology by immunizing mice with sublethal inocula of two XDR clinical isolates of *A. baumannii* (VA-Ab59 and VA-Ab65) obtained from patients at the Louis B. Stokes Veterans Affairs Hospital in Cleveland, Ohio, to which our initial MAb C8 did not bind (12). After confirming that the initial murine IgM bound to both immunizing strains of *A. baumannii* by flow cytometry, we then humanized and isotype-switched the MAb to IgG1, calling it MAb 65. When tested by flow cytometry, MAb 65 bound as well as immune serum to the surface of VA-Ab41, an XDR clinical isolate of *A. baumannii* from a skin and soft-tissue infection that is hypervirulent in mice (Fig. 1A). Strong surface binding of MAb 65 to VA-Ab41 was observed by flow cytometry at concentrations as low as 100 ng/ml. We then assessed the ability of MAb 65 to bind to a broad collection of 302 clinical isolates of *A. baumannii*, originating from a wide variety of infection types, from across the United States. By flow cytometry, surface binding by MAb 65 was significantly greater than that of negative isotype control antibody in 70 of the 302 (23%) *A. baumannii* strains tested. Thirty-six (51%) of the strains bound by MAb 65 were not bound by our first MAb, which had previously been tested against only 95 strains, and has subsequently been tested against the additional isolates for the current study (11). Combined with the original MAb C8 and the new MAb 65, 119 of 302 isolates (39%) are bound by either MAb.

Using Western blotting, we previously observed with MAb C8 that bacterial binding was eliminated by treating bacterial surface structures with periodate while remaining unaffected by proteinase K treatment, indicating an entirely carbohydrate target that is consistent with a capsular epitope (11). Using ELISA, an alternative technique, we observed only minimal reduction in binding with proteinase K treatment, whereas binding by our new MAb 65 vanished when treating bacterial surface structures with periodate (Fig. 1B). This indicated a target composed of carbohydrate that may be reinforced or supported by protein structures but not a glycosylated protein. Confocal immunofluorescence microscopy confirmed diffuse binding of MAb 65 to the surface of the *A. baumannii* strain VA-Ab41 (Fig. 1C), identical to binding of our prior MAb C8 to the capsule of HUMC1, another *A. baumannii* clinical isolate tested (11).

MAb 65 enhances macrophage uptake of *A. baumannii* via opsonophagocytosis. VA-Ab41 and HUMC1 *A. baumannii* strains are considered hypervirulent, previously defined (10) as having the ability to evade innate immune effector-mediated clearance from the blood within the first hour of a bloodstream infection at a relatively low inoculum (i.e., 2×10^7 CFU/mouse). Clearance of *A. baumannii* occurs primarily by macrophages and, to a lesser extent, by neutrophils and complement (10, 13). As such, we investigated how well MAb 65 opsonizes *A. baumannii* for macrophage uptake *in vitro*. MAb 65 significantly enhanced the internalization of these two hypervirulent *A. baumannii* strains (VA-Ab41 and HUMC1) by RAW 264.7 macrophage cells, regardless of whether serum was heat inactivated or complement active (Fig. 2A to C).

MAb 65 rescues mice with *A. baumannii* bacteremia. When mice were infected intravenously (i.v.) with 2×10^7 CFU of the XDR hypervirulent *A. baumannii* strain VA-Ab41 and treated i.v. with 5 μ g isotype control or MAb 65, 75% of mice treated with

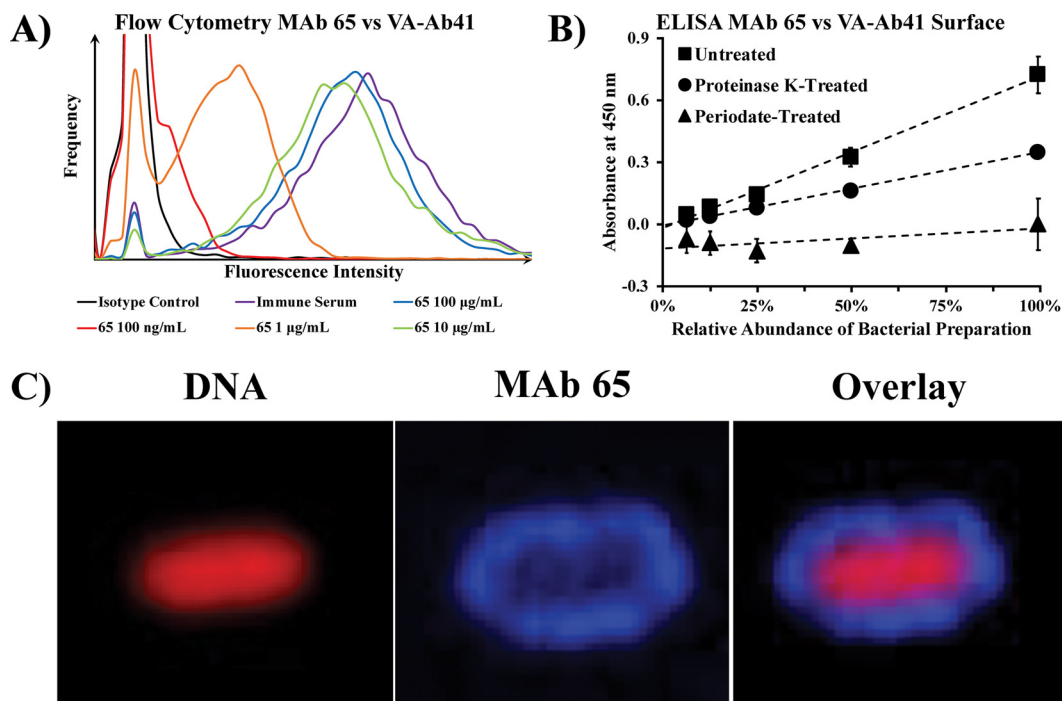


FIG 1 Surface binding of *A. baumannii* by purified MAb 65. (A) *A. baumannii* VA-Ab41 bacteria grown to log phase were stained with various concentrations of purified MAb 65 (primary antibody), followed by fluorophore-conjugated anti-human IgG heavy and light chain (polyclonal secondary antibody), to assess MAb binding by flow cytometry. Binding of polyclonal immune serum from the immunized mice euthanized to create hybridomas was used as a positive control. (B) ELISA of MAb 65 binding to capsule preparations of *A. baumannii*, including capsule preparations left untreated, treated with proteinase K to degrade protein, or treated with periodate to degrade carbohydrates. The plot includes linear trend lines of averages with standard deviation error bars. (C) Confocal immunofluorescence microscopy confirmed diffuse surface binding of MAb 65 (rhodamine, blue) to DNA-stained (Cy5, red) *A. baumannii* VA-Ab41.

isotype control succumbed to the infection, whereas the same percentage of mice treated with MAb 65 survived (Fig. 3A). When we repeated the experiment with double the inoculum, all mice treated with 50 µg isotype control died, whereas all mice treated with 50 µg MAb 65 survived (Fig. 3B).

Since clinical treatment of *A. baumannii* infections using antibody therapy will likely occur in conjunction with antibiotic treatment, we assessed the efficacy of administering MAb treatment in combination with colistin. At a high inoculum, MAb 65 and colistin monotherapies improved survival compared to the isotype control but still resulted in more than half of the mice dying (Fig. 3C). In contrast, combination therapy was synergistic, resulting in complete protection against lethal bacteremia (Fig. 3C). Moreover, clinical treatment may involve delayed time to onset of therapy. Mice treated 30 min or 1 h postinfection intraperitoneally (i.p.) with 100 µg MAb 65 survived, whereas those treated immediately with isotype control succumbed to the infection (Fig. 3D).

Treatment with MAb 65 reduced bacterial burden and prevented the onset of sepsis. To determine the mechanism by which MAb 65 protects from lethal bacteremia, we studied the impact of MAb treatment on bacterial density and sepsis syndrome in mice challenged with *A. baumannii*. Mice were infected i.v. via the tail vein with VA-Ab41 and then treated i.v. with 10 µg isotype control or MAb 65. At 2 h postinfection, mice treated with MAb 65 had a 75% reduction of bacterial density in their blood compared to mice treated with the isotype control (Fig. 4A). During the ensuing 16 h, bacterial density in the blood of mice treated with MAb 65 declined 2.9-log₁₀-fold, whereas mice treated with isotype control experienced a decline of only 0.9-log₁₀-fold (Fig. 4A).

Proinflammatory (interleukin-1β [IL-1β], IL-6, and tumor necrosis factor [TNF]) and anti-inflammatory (IL-10) cytokines were also dramatically different in mice treated

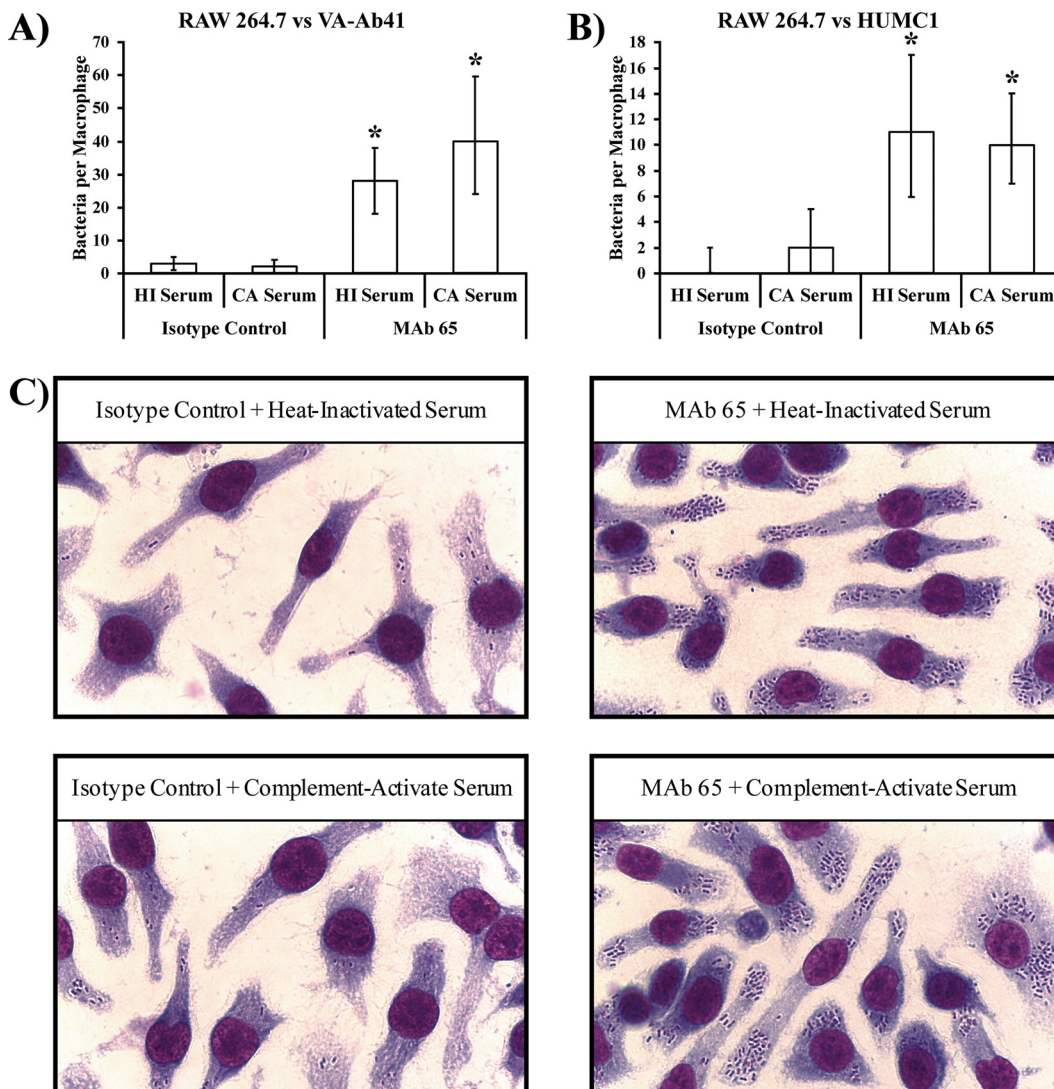


FIG 2 MAb 65 opsonizes *A. baumannii* for macrophage uptake. (A and B) RAW 264.7 murine macrophage cells were ineffective at taking up *A. baumannii* in the absence of complement or MAb 65. In the presence of complement-active CD-1 mouse serum (CA serum), macrophages were no more capable of taking up bacteria than heat-inactivated CD-1 mouse serum (HI serum). However, the addition of MAb 65 (20 μ g/ml) significantly improved the ability of macrophages to take up bacteria, regardless of whether the complement was active or heat inactivated. Median and interquartile ranges are shown. *, $P < 0.05$ compared to isotype control groups by the Wilcoxon rank sum test for unpaired comparisons. (C) Hema-3 staining reveals the dramatic increase in macrophage internalization of VA-Ab41 bacteria upon addition of 20 μ g/ml MAb 65.

with MAb 65 compared to mice treated with isotype control (Fig. 4B). TNF was highly elevated in mice treated with isotype control by 2 h postinfection and significantly lower in mice treated with MAb 65 (Fig. 4B). Conversely, IL-10 was significantly elevated in mice treated with MAb 65 by 2 h postinfection and returned to baseline by 18 h postinfection, whereas levels of the cytokine remained flat for mice treated with isotype control (Fig. 4B). By 18 h postinfection, IL-6 had significantly diminished in mice treated with MAb 65 but not in mice treated with isotype control (Fig. 4B).

Sepsis biomarkers were congruent with cytokine profiles and blood bacterial densities, including renal failure based on hypoglycemia (low blood glucose) and elevated blood urea nitrogen (BUN), consistent with septic shock syndrome in mice treated with isotype control but not in mice treated with MAb 65 (Fig. 4C).

MAb 65 protects against lethal *A. baumannii* pneumonia. We further tested the efficacy of MAb 65 in another clinically relevant *in vivo* model of infection: an aspiration

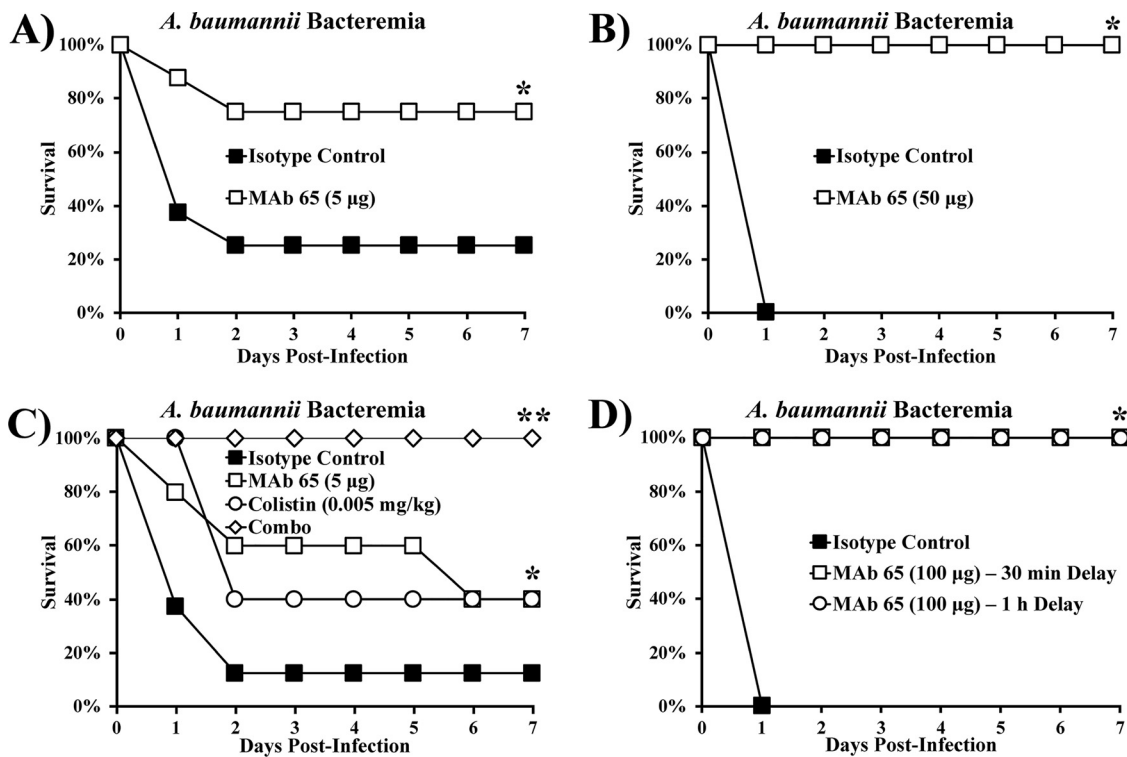


FIG 3 MAb 65 rescues mice with *A. baumannii* bacteremia. Mice were infected i.v. via the tail vein with the XDR hypervirulent *A. baumannii* strain VA-Ab 41 and treated with MAb 65. (A) Most mice infected with 2×10^7 CFU could not clear the infection if treated with $5 \mu\text{g}$ isotype control, but most mice survived when treated with $5 \mu\text{g}$ MAb 65. $N=8$ mice/group; *, $P < 0.05$ versus isotype control group by the nonparametric log rank test. (B) All mice infected with 4×10^7 CFU succumbed to the infection if treated with $50 \mu\text{g}$ isotype control, but all mice survived when treated with $50 \mu\text{g}$ MAb 65. $N=7$ mice/group; *, $P < 0.05$ versus isotype control group by the nonparametric log rank test. (C) Mice were mostly unable to survive an infection with 5×10^7 CFU when treated with $5 \mu\text{g}$ isotype control, fewer than half survived with a single dose of 0.005 mg/kg colistin or $5 \mu\text{g}$ MAb 65 monotherapy, and all survived with the combination of colistin and MAb 65 treatment. $N=8$ mice/group for isotype control group and 5 mice/group for MAb 65, colistin, and combination groups; *, $P < 0.05$ versus isotype control group; **, $P < 0.05$ versus all groups by the nonparametric log rank test. (D) Mice treated 30 min or 1 h postinfection intraperitoneally (i.p.) with $100 \mu\text{g}$ MAb 65 survived, whereas mice treated with $100 \mu\text{g}$ isotype control did not survive. $N=5$ mice/group; *, $P < 0.05$ versus isotype control group by the nonparametric log rank test.

pneumonia model that recapitulates the most common clinical presentation of *A. baumannii* infection (14). Administration of $100 \mu\text{g}$ MAb 65 i.v. was protective against aspiration pneumonia (Fig. 5A). MAb 65 was also able to clear nearly all bacteria from both the lungs and the blood by 48 h postinfection, whereas mice treated with isotype control experienced increased blood bacterial burden and no change in lung bacterial burden (Fig. 5B and C). When examined by immunohistochemical staining to highlight the presence of intrapulmonary bacteria, the effects of bacterial burden in the lungs were unclear by 2 h postinfection but were clearly greater in the mice treated with isotype control compared to mice treated with MAb 65 at 24 h postinfection (Fig. 5D). By 2 h postinfection, lungs from mice treated with the isotype control began to demonstrate thickened intralobular septa and early alveolar consolidation, as visible on high-power microscopy (Fig. 5D). At 24 h postinfection, lungs from mice treated with isotype control demonstrated severe hemorrhagic alveolar consolidation, while lungs from mice treated with MAb 65 appeared more normal (Fig. 5D).

Serial passaging with MAb 65 did not diminish its binding capacity. We serially passaged *A. baumannii* VA-Ab41 with isotype control or MAb 65 to evaluate whether escape mutants might arise. Serially passaging the bacteria to log phase 20 times did not result in loss of the MAb 65 binding site. Flow cytometry showed no difference in the degree of MAb 65 binding to VA-Ab41 after being serially passaged in the isotype control (Fig. 6A) or MAb 65 (Fig. 6B). Opsonophagocytosis of VA-Ab41 by RAW 264.7

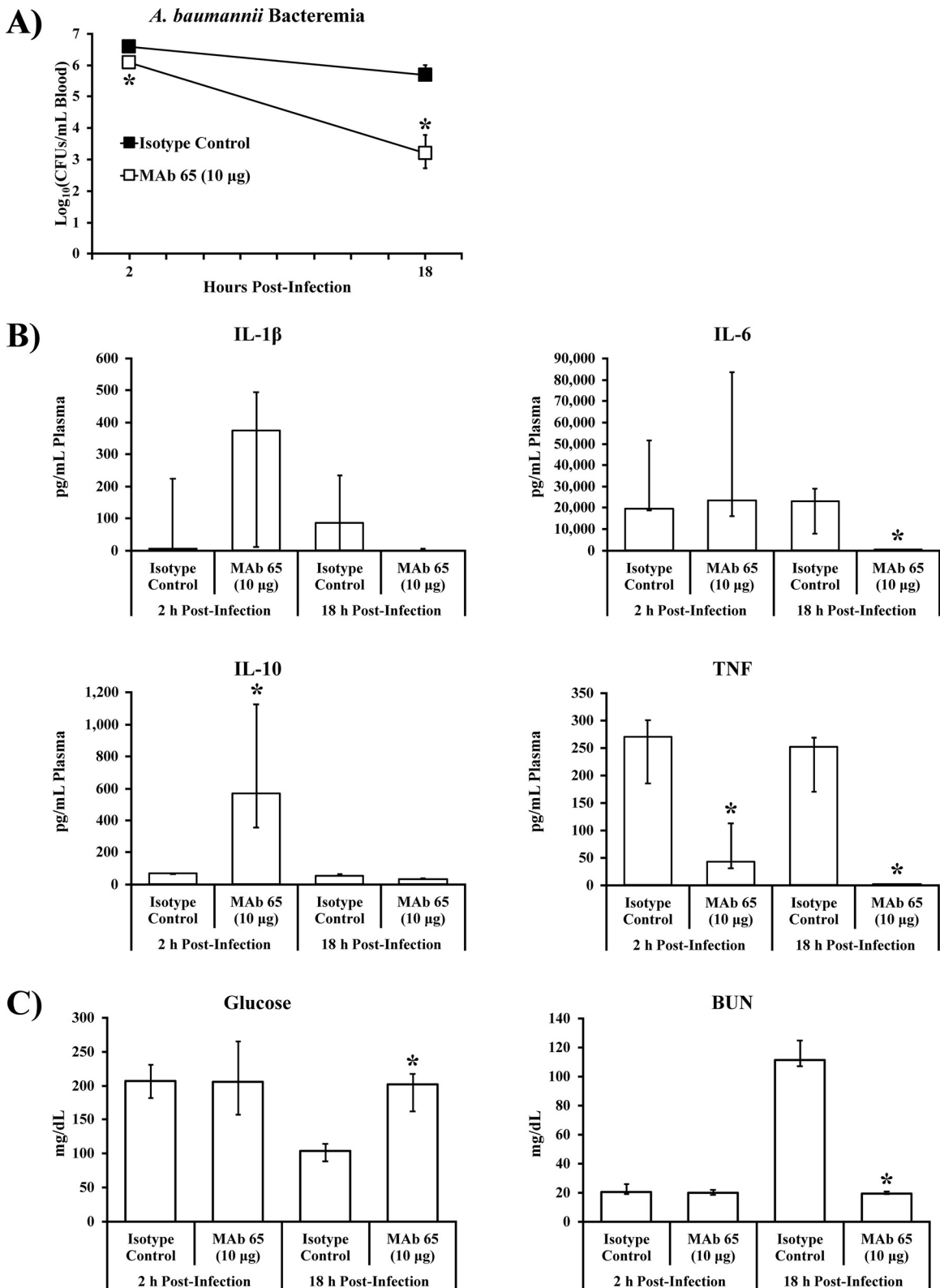


FIG 4 MAb 65 ameliorates bacterial burden, cytokine profile, and sepsis biomarkers during *A. baumannii* bacteremia. (A and B) Bacterial burden (A) and cytokines (B) of mice infected i.v. via tail vein with 2×10^7 CFU *A. baumannii* VA-Ab 41 and treated with 10 µg isotype control or MAb 65; blood plasma was assessed for cytokine levels by Luminex assay. (C) Sepsis biomarkers were congruent with cytokine profiles and blood bacterial densities; blood plasma was assessed for biomarkers of sepsis by iSTAT. $N=5$ to 6 mice/group; *, $P < 0.05$ compared to isotype control group at same time point postinfection by the Wilcoxon rank-sum test for unpaired comparisons; medians and interquartile ranges are shown.

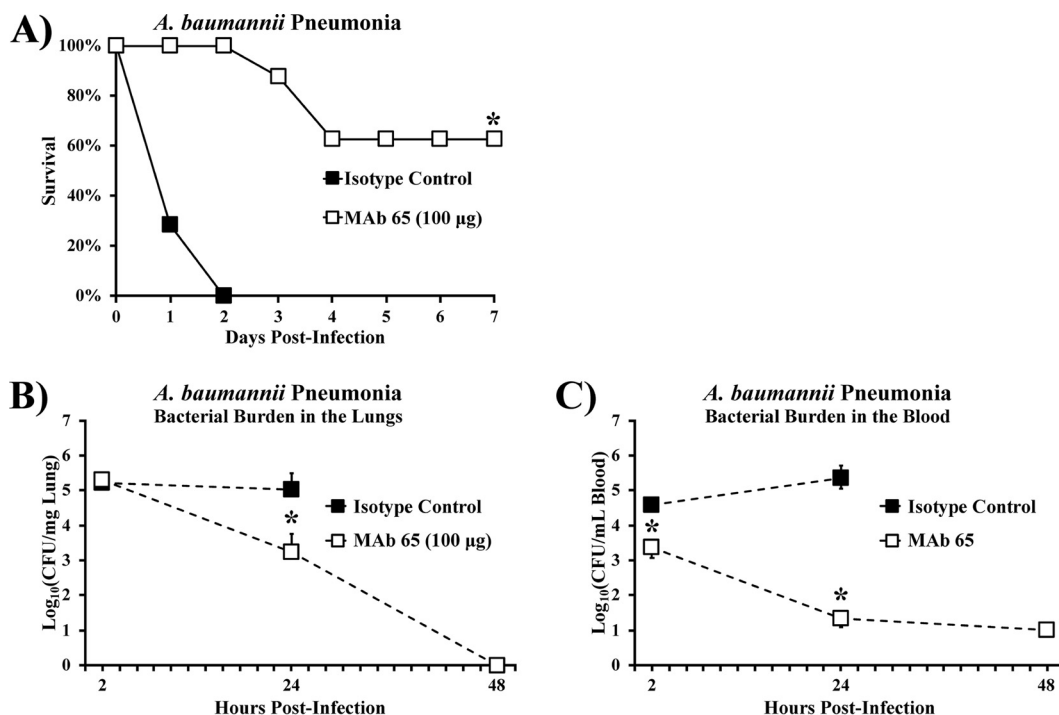


FIG 5 MAb 65 rescues mice with *A. baumannii* aspiration pneumonia. Mice were challenged via oral aspiration with 2×10^7 CFU VA-Ab41 and treated i.v. with 100 μ g MAb 65 or isotype control. (A) Most mice survived aspiration pneumonia when treated with MAb 65. $N=7$ to 8 mice/group; *, $P < 0.05$ versus isotype control group by the nonparametric log rank test. Mice treated with MAb 65 experienced a decrease in bacterial burden in the lungs (B) and blood (C) by 24 h postinfection, with nearly undetectable levels of bacteria by 48 h postinfection. $N=5$ mice/group; *, $P < 0.05$ versus isotype control group by the Wilcoxon rank-sum test for unpaired comparisons; medians and interquartile ranges are shown. (D) Lung architecture was consistent with these findings.

macrophages with MAb 65 was no different between the parent strain and those passaged in either isotype control or MAb 65 (Fig. 6C). Finally, MAb 65 was still able to rescue mice infected with VA-Ab41 that had been passaged in the presence of MAb 65 (Fig. 6D). Therefore, serial passaging did not lead to escape mutants.

DISCUSSION

A. baumannii is among the most antibiotic-resistant pathogens now encountered in clinical medicine (15). Identifying new therapies is greatly needed, particularly with the paucity of novel antibiotics under development to treat infections caused by this organism. We have now identified a second immunotherapeutic, MAb 65, that binds to a carbohydrate moiety on the surface of *A. baumannii*. The repertoire of strains bound by MAb 65 complements that of our first monoclonal antibody, MAb C8, greatly increasing the likelihood that a clinical *A. baumannii* infection will be recognized by our immunotherapy. Both MAbs are highly effective at rescuing mice from lethal bacteremia and pneumonia caused by hypervirulent XDR *A. baumannii* clinical isolates. Furthermore, both MAbs work synergistically in combination with colistin, which is the current standard of care for treatment-resistant *A. baumannii* infections. These results pave the way for clinical development in the setting of immunotherapy as an adjunct treatment with standard-of-care antibiotics.

There has been recent success in the development of a multivalent immunotherapy that protects against the highly drug-resistant bacterial species *Pseudomonas aeruginosa* (16), demonstrating promising results in a recent phase 1 study (17). Future studies of this immunotherapy for the treatment of *A. baumannii* infections will investigate the combination of multiple monoclonal antibodies versus multivalent antibodies to treat infections of *A. baumannii*. Additionally, a lead candidate for passive immunization will need to be screened for toxicity against human tissues after establishing GMP production. These two MAbs are highly complementary and, together, bind to 39% of a diverse collection of 302 *A. baumannii* strains tested. Therefore, three or four MAbs may be required to achieve 80

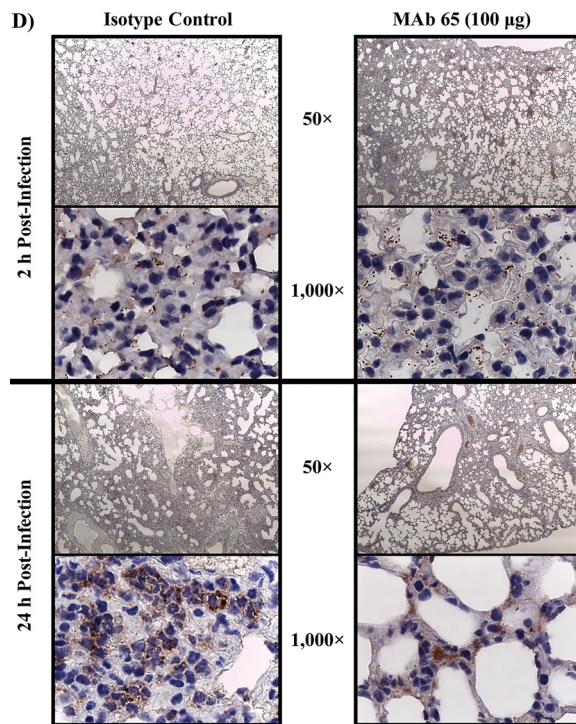


FIG 5 (Continued)

to 90% strain coverage to enable empirical therapy without necessitating a diagnostic assay to identify which clinical strains are bound by the MABs.

In conclusion, we have now developed two MABs that rescue mice from blood and lung infections caused by hypervirulent, XDR clinical isolates of *A. baumannii*. Both MABs have been successfully humanized and are able to opsonize bacteria for phagocytic clearance, modulate the release of inflammatory cytokines to improve survival, and function synergistically with the antibiotic colistin. These MABs may be useful as part of a multivalent therapeutic regimen to treat antibiotic-resistant *A. baumannii* infections.

MATERIALS AND METHODS

Generation of hybridomas. To generate hybridomas, we performed primary immunizations by infecting mice intravenously with a small, sublethal inoculum (5×10^4 CFU) of viable *A. baumannii* VA-Ab59 bacteria. Secondary immunizations followed 3 weeks later with the capsule extract of VA-Ab65 injected i.v., and tertiary immunizations followed 3 months after the secondary immunizations with the same capsule extract, this time injected i.p. Two weeks following the last boost and 3 days before harvesting of spleens for hybridoma fusion, we injected mice subcutaneously with $50 \mu\text{g}$ anti-mouse CD40 MAb (clone 5C3; BioLegend) (18). Hybridoma cell lines were propagated in 96-well, flat-bottom plates in Dulbecco's modified Eagle medium supplemented with 20% fetal bovine serum (DMEM-20). Supernatants were harvested from wells for initial screening by flow cytometry to identify antibodies that bound to intact bacteria. Subcloned monoclonal hybridomas were slowly transitioned from DMEM-20 to protein-free hybridoma medium (Life Technologies). Antibodies were purified from monoclonal hybridoma supernatants using protein G-agarose resin (ThermoFisher Scientific) per the manufacturer's instructions. Isotype was determined by a BD Pharmingen mouse immunoglobulin isotyping ELISA kit (ThermoFisher Scientific).

Development of the humanized MAB. The humanized IgG1 MAB was developed by Precision Antibody using their well-established methodology. In brief, MAB 65 heavy- and light-chain variable regions were identified by reverse transcription-PCR (RT-PCR) using the Novagen mouse Ig degenerate primer set per the manufacturer's instructions. Light- and heavy-chain variable regions were aligned with the murine germ line sequences from which they were derived and their human analogs. Humanized variable regions were electronically grafted to human IgG1 heavy- and light-chain constant regions and synthesized in mammalian expression vectors at GenScript.

Bacterial strains. HUMC1, VA-Ab41, VA-Ab59, and VA-Ab65 are *A. baumannii* clinical skin and soft-tissue infection isolates that are extremely drug resistant (XDR). HUMC1 and VA-Ab41 are hypervirulent in our murine bacteremia model (i.e., an inoculum of $<5 \times 10^7$ CFU is lethal to all mice) (8–10, 19).

Bacterial binding by flow cytometry. To assess surface binding of antibodies, *A. baumannii* subcultures were passaged for 3 h to mid-log-phase growth, rinsed three times in phosphate-buffered saline (PBS), and then resuspended in PBS supplemented with 0.1% NaN_3 to prevent contamination of the flow

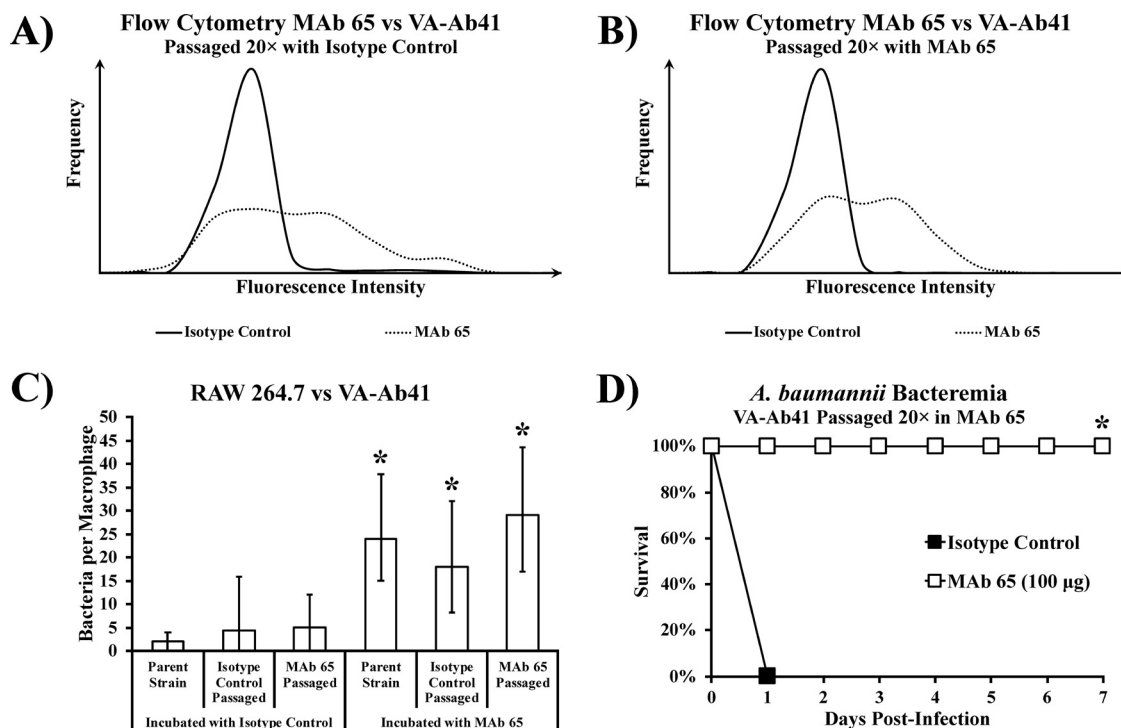


FIG 6 Bacteria retain binding site after being serially passaged with MAb 65. Flow cytometry showed little difference in the degree of MAb 65 binding to VA-Ab41 after serially passaging the strain 20 times with isotype control (A) or MAb 65 (B). (C) MAb 65 induced similar levels of opsonophagocytosis in RAW 264.7 murine macrophages in the presence of VA-Ab41, regardless of whether it was the parent strain, passaged in the isotype control, or passaged in MAb 65; medians and interquartile ranges are shown. *, $P < 0.05$ compared to strains incubated with isotype control by the Wilcoxon rank-sum test for unpaired comparisons. (D) Mice infected i.v. with 1×10^8 CFU VA-Ab41 passaged 20 times in the presence of MAb 65 were still able to be rescued with $100 \mu\text{g}$ MAb 65. *, $P < 0.05$ versus isotype control group by the nonparametric log rank test.

cytometer. Hybridoma supernatant or purified MAb was added to each well, gently mixed with a plate vortexer, and incubated for 30 min at 37°C . Bacteria were then washed and transferred to 5-ml tubes in PBS. Flow cytometry was conducted on a CANTO II Cytometer (BD) with staining by AF647-conjugated anti-human IgG secondary antibody.

Target identification. To identify the target of the MAb, we made a bacterial surface preparation, as described previously (20–22). In brief, we grew an overnight culture of *A. baumannii* VA-Ab41 in tryptic soy broth, centrifuged it at $4,000 \times g$ for 5 min, and extracted capsular polysaccharide with ethylenediaminetetraacetic acid and then phenol. An ELISA was run with the bacterial capsular polysaccharide either untreated, treated with 0.25 M sodium periodate (NaIO_4) to degrade polysaccharides, or treated with 10 mg/ml proteinase K to degrade polypeptides.

Confocal immunofluorescence microscopy. To detect surface binding of *A. baumannii* by purified MAb 65, frozen bacteria were fixed with 4% paraformaldehyde (PFA) in PBS for 5 min, rinsed three times with PBS, blocked for 15 min in PBS with 1% bovine serum albumin (BSA; 23209; ThermoFisher) and 0.1% Triton X (AAA16046-AE; VWR), and then incubated with $10 \mu\text{g}/\text{ml}$ primary antibody for 1 h at 37°C . Bacteria were then rinsed with PBS and blocked in PBS with 10% goat serum (50062Z; ThermoFisher) for 10 min at room temperature. Samples were then incubated with $10 \mu\text{g}/\text{ml}$ secondary antibody (A21445; ThermoFisher) diluted in PBS for 45 min at room temperature. The bacteria were then placed in a mounting medium containing propidium iodide (101098-046; VWR) and imaged by confocal microscopy (Perkin Elmer Ultraview spinning disc confocal microscope).

In vitro macrophage opsonophagocytosis assays. To measure opsonophagocytosis, we used RAW 264.7 murine macrophages ($5 \times 10^5/\text{well}$; ATCC) stimulated with 100 U/ml gamma interferon overnight, as we previously described (23). Cells adhered to the cover glass overnight in a humidified incubator at 37°C supplemented with 5% CO_2 . Bacteria were prepared from overnight cultures of *A. baumannii* subcultured to log phase, washed in PBS, and resuspended in Hanks' balanced salt solution (HBSS) to 2×10^8 CFU/ml. Cells were rinsed three times with HBSS, and bacteria were added to wells at a ratio of 20:1 (bacteria to macrophages) in the presence (or absence) of 10% CD-1 (IMSCD1-COMPL; Innovative Research Inc.) mouse serum that was either complement active or heat inactivated. Macrophages were washed three times with HBSS, fixed with 100% methanol, and Hema-3 stained according to the manufacturer's protocol (Fisher Scientific). To quantitate bacteria per macrophage, coverslips were imaged on a Leica DMLS clinical microscope with a Leica ICC50 HD digital camera.

Bacterial inoculum preparation. Bacteria were grown overnight in tryptic soy broth (TSB) at 37°C with shaking at 200 rpm. The bacteria were passaged to mid-log growth phase in TSB at 37°C with shaking at 200 rpm for 3 h. Subcultures were rinsed three times with PBS and resuspended in PBS. To reduce variability

between inocula, identical aliquots of PBS-suspended subcultures were stored frozen at -80°C , thawed for use when needed, and diluted with PBS to the appropriate concentration, as we have previously described (24). During all *in vivo* experiments, the inoculum is delivered prior to treatment.

Mouse models of infection. C3HeB/Fe (wild type; strain 000658) mice were purchased from Jackson Laboratories and used for survival, bacterial burden, and cytokine studies, as we have previously described for *A. baumannii* infection (7, 8, 10). Mice were between 9 and 12 weeks of age at the time of infection and weighed approximately 30 g.

For the bloodstream infection model, mice were infected i.v. via the tail vein with designated inocula of *A. baumannii* isolates. For the pneumonia model, an oropharyngeal model of aspiration pneumonia that recapitulates hospital- or ventilator-associated pneumonia (relevant to intensive care unit populations) was used (14). In brief, mice were sedated with isoflurane and hung by their maxillary incisors, tongues were held to prevent swallowing, and $50\ \mu\text{l}$ bacterial inoculum was placed in the trachea to allow inoculation of the bacteria into the lungs by reflexive aspiration.

For colistin treatment, colistin sulfate salt (C4461; Sigma) was dissolved in PBS to $0.6\ \mu\text{g}/\text{ml}$ and $250\ \mu\text{l}$ delivered i.p. to each $\sim 30\text{-g}$ mouse for a dose of $0.005\ \text{mg}/\text{kg}$ of body weight.

All animal work was conducted following approval by the Institutional Animal Care and Use Committee (IACUC) at the University of Southern California, in compliance with the recommendations in the *Guide for the Care and Use of Laboratory Animals* (25) of the National Institutes of Health, IACUC protocol numbers 20208 and 20750.

Immunohistochemical staining. Lung tissue from mice infected with *A. baumannii* and treated with humanized antibody was harvested, fixed, processed, and embedded in paraffin to create formalin-fixed paraffin-embedded (FFPE) tissue, per standard protocols. Slides for immunohistochemistry were cut at a thickness of 3 to $5\ \mu\text{m}$ and baked at 60°C for 1 h; immunostaining was performed using a Bond-III automated immunostainer (Leica Biosystems). Preincubation steps included xylene dewaxing for 8 min, washing with PBS for 10 min, heat-induced epitope retrieval (HIER) using Bond epitope retrieval solution 2 (Leica Biosystems) for 30 min at 100°C , and washing slides with PBS for 10 min. Slides were incubated with mouse polyclonal serum at 1:500 for 1 h at room temperature. Slides were washed with PBS for 10 min. A MACH 2 rabbit horseradish peroxidase (HRP) polymer detection system (Biocare Medical, LLC) and 3,3'-diaminobenzidine (DAB) based chromogen kit (Bond polymer refine detection; Leica Biosystems) were employed for secondary detection per the manufacturer's directions. Slides were dehydrated in alcohol (95% ethanol for 2 min, 100% ethanol for 2 min), returned to xylene, and cover-slipped using standard mounting medium (Surgipath Micromount; Leica Biosystems).

Statistics. Survival was compared by the nonparametric log rank test. Bacteria per macrophage, bacterial burden in lungs and blood, cytokines, and biomarkers were compared with the Wilcoxon rank sum test for unpaired comparisons. All statistics were run using STATA software version 15. Differences were considered significant if the *P* value was ≤ 0.05 .

ACKNOWLEDGMENTS

This work was supported by the National Institute of Allergy and Infectious Diseases at the National Institutes of Health (grant numbers R01 AI130060, R01 AI117211, R21 AI127954, and R42 AI106375 to B.S.; R01 AI139052 to B.M.L.; R01 AI100560, R01 AI063517, and R01 AI072219 to R.A.B.). This study was also supported in part by funds and/or facilities provided by the Cleveland Department of Veterans Affairs, award number 1101BX001974, to R.A.B. from the Biomedical Laboratory Research & Development Service of the VA Office of Research and Development and the Geriatric Research Education and Clinical Center VISN 10.

The content is solely the responsibility of the authors and does not necessarily represent the official views of the National Institutes of Health or the Department of Veterans Affairs.

T.B.N. and B.S. are inventors on a patent related to MAb 65. T.B.N. and B.S. own equity in BioAIM, which is developing the MAb. U.S.C. has an ownership interest in BioAIM and is entitled to a share of royalties based on a licensing agreement with BioAIM. There are no other conflicts.

REFERENCES

- Spellberg B, Rex JH. 2013. The value of single-pathogen antibacterial agents. *Nat Rev Drug Discov* 12:963. <https://doi.org/10.1038/nrd3957-c1>.
- Shlaes DM, Sahn D, Opiela C, Spellberg B. 2013. Commentary: the FDA reboot of antibiotic development. *Antimicrob Agents Chemother* 57:4605–4607. <https://doi.org/10.1128/AAC.01277-13>.
- Weiner LM, Webb AK, Limbago B, Dudeck MA, Patel J, Kallen AJ, Edwards JR, Sievert DM. 2016. Antimicrobial-resistant pathogens associated with healthcare-associated infections: summary of data reported to the National Healthcare Safety Network at the Centers for Disease Control and Prevention, 2011–2014. *Infect Control Hosp Epidemiol* 37:1288–1301. <https://doi.org/10.1017/ice.2016.174>.
- Hu FP, Guo Y, Zhu DM, Wang F, Jiang XF, Xu YC, Zhang XJ, Zhang CJP, Xie Y, Kang M, Wang CQ, Wang AM, Xu YH, Shen JL, Sun ZY, Chen ZJ, Ni YX, Sun JY, Chu YZ, Tian SF, Hu ZD, Li J, Yu YS, Lin J, Shan B, Du Y, Han Y, Guo S, Wei LH, Wu L, Zhang H, Kong J, Hu YJ, Ai XM, Zhuo C, Su DH, Yang Q, Jia B, Huang W. 2016. Resistance trends among clinical isolates in China reported from CHINET surveillance of bacterial resistance, 2005–2014. *Clin Microbiol Infect* 22(Suppl 1):S9–S14. <https://doi.org/10.1016/j.cmi.2016.01.001>.

5. Spellberg B, Guidos R, Gilbert D, Bradley J, Boucher HW, Scheld WM, Bartlett JG, Edwards J, Jr, Infectious Diseases Society of America. 2008. The epidemic of antibiotic-resistant infections: a call to action for the medical community from the Infectious Diseases Society of America. *Clin Infect Dis* 46:155–164. <https://doi.org/10.1086/524891>.
6. Butler MS, Blaskovich MA, Cooper MA. 2013. Antibiotics in the clinical pipeline in 2013. *J Antibiot* 66:571–591. <https://doi.org/10.1038/ja.2013.86>.
7. Lin L, Tan B, Pantapalangkoor P, Ho T, Hujer AM, Taracila MA, Bonomo RA, Spellberg B. 2013. Acinetobacter baumannii rOmpA vaccine dose alters immune polarization and immunodominant epitopes. *Vaccine* 31:313–318. <https://doi.org/10.1016/j.vaccine.2012.11.008>.
8. Lin L, Tan B, Pantapalangkoor P, Ho T, Baquir B, Tomaras A, Montgomery JI, Reilly U, Barbacci EG, Hujer K, Bonomo RA, Fernandez L, Hancock RE, Adams MD, French SW, Buslon VS, Spellberg B. 2012. Inhibition of LpxC protects mice from resistant Acinetobacter baumannii by modulating inflammation and enhancing phagocytosis. *mBio* 3:e00312-12. <https://doi.org/10.1128/mBio.00312-12>.
9. Luo G, Lin L, Ibrahim AS, Baquir B, Pantapalangkoor P, Bonomo RA, Doi Y, Adams MD, Russo TA, Spellberg B. 2012. Active and passive immunization protects against lethal, extreme drug resistant-Acinetobacter baumannii infection. *PLoS One* 7:e29446. <https://doi.org/10.1371/journal.pone.0029446>.
10. Bruhn KW, Pantapalangkoor P, Nielsen T, Tan B, Junus J, Hujer KM, Wright MS, Bonomo RA, Adams MD, Chen W, Spellberg B. 2015. Host fate is rapidly determined by innate effector-microbial interactions during Acinetobacter baumannii bacteremia. *J Infect Dis* 211:1296–1305. <https://doi.org/10.1093/infdis/jiu593>.
11. Nielsen TB, Pantapalangkoor P, Luna BM, Bruhn KW, Yan J, Dekitani K, Hsieh S, Yeshoua B, Pascual B, Vinogradov E, Hujer KM, Domitrovic TN, Bonomo RA, Russo TA, Leszczyniecka M, Schneider T, Spellberg B. 2017. Monoclonal antibody protects against Acinetobacter baumannii infection by enhancing bacterial clearance and evading sepsis. *J Infect Dis* 216:489–501. <https://doi.org/10.1093/infdis/jix315>.
12. Campodonico VL, Llosa NJ, Grout M, Doring G, Maira-Litran T, Pier GB. 2010. Evaluation of flagella and flagellin of Pseudomonas aeruginosa as vaccines. *Infect Immun* 78:746–755. <https://doi.org/10.1128/IAI.00806-09>.
13. Luna BM, Yan J, Reyna Z, Moon E, Nielsen TB, Reza H, Lu P, Bonomo R, Louie A, Drusano G, Bulitta J, She R, Spellberg B. 2019. Natural history of Acinetobacter baumannii infection in mice. *PLoS One* 14:e0219824. <https://doi.org/10.1371/journal.pone.0219824>.
14. Nielsen TB, Yan J, Luna B, Spellberg B. 2018. Murine oropharyngeal aspiration model of ventilator-associated and hospital-acquired bacterial pneumonia. *J Vis Exp* 2018:57672. <https://doi.org/10.3791/57672>.
15. Wong D, Nielsen TB, Bonomo RA, Pantapalangkoor P, Luna B, Spellberg B. 2017. Clinical and pathophysiological overview of Acinetobacter infections: a century of challenges. *Clin Microbiol Rev* 30:409–447. <https://doi.org/10.1128/CMR.00058-16>.
16. DiGiandomenico A, Keller AE, Gao C, Rainey GJ, Warrenner P, Camara MM, Bonnell J, Fleming R, Bezabeh B, Dimasi N, Sellman BR, Hilliard J, Guenther CM, Datta V, Zhao W, Gao C, Yu XQ, Suzich JA, Stover CK. 2014. A multifunctional bispecific antibody protects against Pseudomonas aeruginosa. *Sci Transl Med* 6:262ra155. <https://doi.org/10.1126/scitranslmed.3009655>.
17. Ali SO, Yu XQ, Robbie GJ, Wu Y, Shoemaker K, Yu L, DiGiandomenico A, Keller AE, Anude C, Hernandez-Illas M, Bellamy T, Falloon J, Dubovsky F, Jafri HS. 2019. Phase 1 study of MEDI3902, an investigational anti-Pseudomonas aeruginosa PcrV and Psl bispecific human monoclonal antibody, in healthy adults. *Clin Microbiol Infect* 25:629. <https://doi.org/10.1016/j.cmi.2018.08.004>.
18. Ryczyn MA, Staquet K, Fisher J, Bannish G, Bassiri A, Duchala C, Giles-Komar J. 2008. The use of an anti-CD40 agonist monoclonal antibody during immunizations enhances hybridoma generation. *Hybridoma* 27:25–30. <https://doi.org/10.1089/hyb.2007.0537>.
19. Luo G, Spellberg B, Gebremariam T, Bolaris M, Lee H, Fu Y, French SW, Ibrahim AS. 2012. Diabetic murine models for Acinetobacter baumannii infection. *J Antimicrob Chemother* 67:1439–1445. <https://doi.org/10.1093/jac/dks050>.
20. Kubler-Kielb J, Vinogradov E, Ng WI, Maczynska B, Junka A, Bartoszewicz M, Zelazny A, Bennett J, Schneerson R. 2013. The capsular polysaccharide and lipopolysaccharide structures of two carbapenem resistant Klebsiella pneumoniae outbreak isolates. *Carbohydr Res* 369:6–9. <https://doi.org/10.1016/j.carres.2012.12.018>.
21. Vinogradov E, Maclean L, Xu HH, Chen W. 2014. The structure of the polysaccharide isolated from Acinetobacter baumannii strain LAC-4. *Carbohydr Res* 390:42–45. <https://doi.org/10.1016/j.carres.2014.03.001>.
22. Russo TA, Beanan JM, Olson R, MacDonald U, Cox AD, St Michael F, Vinogradov EV, Spellberg B, Luke-Marshall NR, Campagnari AA. 2013. The K1 capsular polysaccharide from Acinetobacter baumannii is a potential therapeutic target via passive immunization. *Infect Immun* 81:915–922. <https://doi.org/10.1128/IAI.01184-12>.
23. Baquir B, Lemaire S, Van Bambeke F, Tulkens PM, Lin L, Spellberg B. 2012. Macrophage killing of bacterial and fungal pathogens is not inhibited by intense intracellular accumulation of the lipoglycopeptide antibiotic oritavancin. *Clin Infect Dis* 54(Suppl 3):S229–S232. <https://doi.org/10.1093/cid/cir921>.
24. Nielsen TB, Bruhn KW, Pantapalangkoor P, Junus JL, Spellberg B. 2015. Cryopreservation of virulent Acinetobacter baumannii to reduce variability of in vivo studies. *BMC Microbiol* 15:252. <https://doi.org/10.1186/s12866-015-0580-8>.
25. National Research Council. 2011. Guide for the care and use of laboratory animals, 8th ed. National Academies Press, Washington, DC.